High-temperature expansion methods for Ising systems with quenched impurities

Ruth V. Ditzian and Leo P. Kadanoff
The James Franck Institute and The Department of Physics, The University of Chicago, Chicago, Illinois 60637
(Received 17 October 1978)

Two methods are used to obtain high-temperature series for Ising systems with quenched randomness. One is a direct averaging of a linked-cluster expansion, the other combines the primitive high-temperature expansion and the Edward replica trick. After a bond renormalization, the second expansion is seen to be identical to the first term by term. The series are developed for the case of a spin-glass model in which the bonds have a probability which is symmetrically distributed about zero. Specifically, series for the free energy and appropriately chosen susceptibility are given to 11th and 10th orders, respectively, for a hypercubic lattice in any dimension and for any symmetrical bond distribution.

I. INTRODUCTION

A. Problem

In this paper, we build upon the work of Fisch,[1] and also that of Fisch and Harris,[2] and of Cherry and Domb[3] to develop high-temperature series for Ising systems with quenched randomness. These authors studied the case in which the probability distribution for a single nearest-neighbor bond $P(J)$ is given by a pair of δ functions at J equal to $\pm|J_1|$. Here we extend these calculations to a general distribution, symmetrical about zero coupling, i.e., a $P(J)$ which obeys

$$P(J)=P(-J) \quad . \tag{1.1}$$

Edwards and Anderson[4] (EA) pointed out that a system with this kind of randomness might be an appropriate model for a spin-glass, with a possible order parameter being $\langle\langle\sigma_i\rangle^2\rangle_{\rm av}$. Here σ_i is an Ising variable at site i, $\langle\ \rangle$ is a statistical average and $\langle\ \rangle_{\rm av}$ is an average over the quenched randomness in the nearest-neighbor interactions J_{ij}. Despite some suggestive calculations,[1-3,5-7] one cannot be quite sure of the nature of the phase transition in this system, namely its lower critical dimension and the kinds of universality classes produced. To help elucidate these questions, we have developed series expansions for the average free energy and for the susceptibility, $\chi_{\rm EA}$, connected with the EA order parameter, which is

$$\chi_{\rm EA}=\sum_{ij}\langle\langle\sigma_i\sigma_j\rangle^2\rangle_{\rm av} \quad . \tag{1.2}$$

B. Series

As one might expect, the natural variables to use in the series are the ones which fully describe the average properties of two Ising spins σ_i and σ_j coupled together with a Hamiltonian $J_{ij}\sigma_i\sigma_j$. These two spins alone would have an average free energy $\ln 4+W_0$, where W_0 is the average

$$W_0=\langle\ln\cosh\beta J_{ij}\rangle_{\rm av}=\int dJ\,P(J)\ln\cosh\beta J \quad . \tag{1.3}$$

Here β is, of course, the inverse temperature in energy units. In addition, the correlation between the two spins is given by

$$\tanh\beta J_{ij}=\langle\sigma_i\sigma_j\rangle_0 \quad . \tag{1.4}$$

(The subscript "0" is a reminder that we are working in a system with only two spins.) Then the key quantities in the expansion are the moments

$$W_m=\langle\langle\sigma_i\sigma_j\rangle_0^m\rangle_{\rm av} =\int dJ\,P(J)(\tanh\beta J)^m \quad . \tag{1.5}$$

By virtue of the symmetry (1.1), the W_m vanish unless m is even.

One can then use the variables defined by Eqs. (1.3) and (1.5) to describe high-temperature series expansions to a given order in the $(J_{ij})^2$. (Note that W_m has a leading order J^m.) In particular in a hypercubic lattice with N sites and dimensionality d the high-temperature series for the average free energy has the form

$$F/N = \ln 2 + dW_0 + \sum_{q,m_2,m_4,m_6} c^q_{m_2,m_4,m_6} \binom{d}{q} W_2^{m_2} W_4^{m_4} W_6^{m_6} , \tag{1.6a}$$

while the susceptibility series is

$$\frac{\chi_{\rm EA}}{N} = 1 + \sum_{q,m_2,m_4,m_6} a^q_{m_2,m_4,m_6} \binom{d}{q} \times W_2^{m_2} W_4^{m_4} W_6^{m_6} . \tag{1.6b}$$

Here the sums over the m's are sums over nonnegative integers and the sum over q starts from 1. Each term has an order which is given by $\frac{1}{2}\sum_j m_j j$. Tables I and II list the principal computational results of this paper, the nonvanishing coefficients c^q_m and a^q_m to respectively 11th and 10th orders.

When these results are specialized to the case of the double δ function used by previous authors[1–3] we discover that they agree for all dimensionalities with the 10th order results previously published. However, as we shall describe below, we made extensive use of the unpublished results of Fisch[1] in obtaining the susceptibility series. There is a disagreement in 11th order in the free energy with the results reported in Ref. 3, but the authors of Ref. 3 now agree with the results presented here.

C. Calculational methodology

The remainder of this paper will be devoted to describing how we obtained the series given in Eqs. (1.6) and Tables I and II. We in fact, employed two different calculational devices, which are separately described in Secs. II and III. In Sec. II, the replica trick[8] is combined with primitive high-temperature expansions as a description of the special case in which $P(J)$ is a Gaussian probability distribution. In Sec. III, a general $P(J)$ is treated via a linked cluster expansion of the impure system.

One of the goals of these two parallel calculations is to make a detailed connection between the replica calculation and the more direct evaluation of the properties of an impure system. From the beginning, we can see a general similarity between the two calculations. They both involve the same general kind of work, i.e., an expansion in skeleton graphs g. As usual,[9] each term is a product of two factors: a lattice constant (g) describing how many graphs of a given type may be fit onto the lattice and a statistical factor f_g describing the weight of one particular graph. In both calculations, one shows that the contribution of disconnected or articulated graphs vanish.

As the next step, the statistical factors f_g are com-

TABLE I. Coefficients $c^q_{P_2P_4}$ are listed with $W_2^{P_2}W_4^{P_4}$ in the first column and $\binom{d}{q}$ labeling the columns.

	$\binom{d}{2}$	$\binom{d}{3}$	$\binom{d}{4}$	$\binom{d}{5}$
W_2^4	$-\frac{1}{2}$			
W_2^6	-1	-8		
W_2^7	4	24		
W_2^8	$-\frac{7}{2}$	-45	-324	
W_2^9	24	584	1600	
W_2^{10}	50	-1344	-8656	-23808
W_2^{11}	108	7656	81792	142080
$W_2^6W_4$	-3	-18		
$W_2^8W_4$	-18	-576	-1152	
$W_2^9W_4$	72	1368	4416	
$W_2^6W_4^2$		-72		
$W_2^7W_4^2$		144		
$W_2^4W_4^3$	-6	-36		
W_4^4	$-\frac{1}{4}$			
$W_2^3W_4^4$	16	96		

TABLE II. Coefficients $a^q_{m_2,m_4,m_6}$ of Eq. (1.6b).

a	q	m_2	m_4	m_6	a	q	m_2	m_4	m_6	a	q	m_2	m_4	m_6
1	1	1			−2 116	2	8			35 712	4	6	1	
1	1	2			6 360	2	8	1		419 328	4	6	2	
1	1	3			−1 064	2	9			201 792	4	7		
1	1	4			−12 580	2	10			5 760	4	7		1
1	1	5			240	3	1	3	1	446 400	4	7	1	
1	1	6			−576	3	1	4		1 199 616	4	8		
1	1	7			144	3	2	3		4 489 344	4	8	1	
1	1	8			−5 472	3	2	4		6 679 424	4	9		
1	1	9			24	3	3			31 697 536	4	10		
1	1	10			144	3	3	2		23 040	5	4	3	
20	2		2	2	1 728	3	3	3		1 920	5	5		
20	2		3	1	216	3	4			23 040	5	5	2	
−48	2		4		144	3	4	1		48 000	5	6		
12	2	1	3		1 728	3	4	2		23 040	5	6	1	
80	2	1	3	1	−4 176	3	4	3		714 240	5	6	2	
−192	2	1	4		1 056	3	5			704 640	5	7		
4	2	2			1 728	3	5	1		714 240	5	7	1	
12	2	2	2		1 440	3	5	1	1	7 977 600	5	8		
48	2	2	3		10 512	3	5	2		13 121 280	5	8	1	
−732	2	2	4		3 456	3	6			77 466 240	5	9		
16	2	3			360	3	6		1	683 297 920	5	10		
12	2	3	1		12 528	3	6	1		23 040	6	6		
48	2	3	2		42 336	3	6	2		345 600	6	6	2	
228	2	3	3		10 680	3	7			829 440	6	7		
24	2	4			2 880	3	7		1	345 600	6	7	1	
48	2	4	1		89 208	3	7	1		17 418 240	6	8		
228	2	4	2		6 360	3	8			14 929 920	6	8	1	
−2088	2	4	3		457 344	3	8	1		280 972 800	6	9		
44	2	5			−6 112	3	9			3 875 535 360	6	10		
228	2	5	1		−634 320	3	10			322 560	7	7		
240	2	5	1	1	−6 912	4	2	4		15 805 440	7	8		
360	2	5	2		1 728	4	3	3		5 806 080	7	8	1	
−116	2	6			192	4	4			447 068 160	7	9		
60	2	6		1	1 728	4	4	2		9 627 125 760	7	10		
696	2	6	1		35 712	4	4	3		5 160 960	8	8		
1392	2	6	2		3 072	4	5			330 301 440	8	9		
−176	2	7			1 728	4	5	1		12 071 485 440	8	10		
120	2	7		1	35 712	4	5	2		92 897 280	9	9		
2628	2	7	1		28 608	4	6			7 524 679 679	9	10		
										1 857 945 600	10	10		

puted for each skeleton diagram as a sum over loops which cover the skeleton diagram. Although at first sight these loop expansions look very different in the two methods, after a simple bond renormalization they are seen to be exactly the same. In this way, we see the term by term identity of the two expansion methods.

II. REPLICA METHOD

A. General method

In dealing with quenched impurities, one must successively calculate two averages; first, the statistical average $\langle\ \rangle$ and then the impurity average.

Edward's replica trick[8] is a device for simplifying the calculation by introducing a new system in which both averages can be performed at the same time. If the original system has a Hamiltonian $H\{\sigma_i, J_{ij}\}$, σ_i being the statistical variables and J_{ij} being the quenched random variables, then the new system contains n replicas of the original one, with new statistical variables σ_i^α ($\alpha = 1, 2, \ldots, n$) and has a Hamiltonian of the form

$$H_{\text{replica}} = \sum_{\alpha=1}^{n} H\{\sigma_i^\alpha, J_{ij}\} + H'\{J_{ij}\}$$
$$= \sum_{\alpha=1}^{n} (H_\alpha + H') \quad . \tag{2.1}$$

In Eq. (2.1), $H'\{J_{ij}\}$ describes the probability distribution for the bonds. In particular, H' is defined so that any function of the bonds $G(J)$ has an average

$$\langle G(J)\rangle_{\text{av}} = \text{Tr}_J e^{-\beta H'\{J\}} G(J) \quad . \tag{2.2}$$

In Eq. (2.2), Tr_J stands for an integral over all possible values of all of the J_{ij}'s.

The statistical mechanics of the quenched system can be directly derived from that of the replica system, in the limit as the number of replicas n, goes to zero. To define this connection, let us use the notation $Z(n)$ to describe the partition function generated by the replica Hamiltonian of Eq. (2.1), i.e.,

$$Z(n) = \text{Tr}_J \text{Tr}_{\sigma_i^\alpha} e^{-\beta H_{\text{replica}}} \quad , \tag{2.3}$$

where $\text{Tr}_{\sigma_i^\alpha}$ represents a sum over all the n statistical variables which lie at the different lattice sites i. Edwards has shown that the average free energy is then given by $\langle f\rangle_{\text{av}}$, where he has

$$-\beta\langle f\rangle_{\text{av}} = \langle F\rangle_{\text{av}} = \lim_{n\to 0} \frac{Z(n)-1}{n} \quad . \tag{2.4}$$

We shall use Eq. (2.4) in generating a high-temperature series expansion for F. At low temperatures, there are problems[10] in using Eq. (2.4). Recent work[11] has shown that these difficulties arise from a natural breaking of the symmetry among replicas. This is not expected at temperatures above the critical. Our work will support this expectation by giving a term by term equivalence between the expansion of the replica system (as given in this section) and the direct linked cluster expansions described in Sec. III.

Correlation functions for the replica system are also directly related to the impurity-averaged correlations. To state this connection imagine that we were interested in calculating some average of the form

$$A = \langle \prod_{k=1}^{q} \langle X_k(\sigma)\rangle\rangle_{\text{av}} \tag{2.5a}$$

in the original system. Here $X_1, X_2, \ldots, X_q$ are different functions of the σ's. Expression (2.5a) is the most general form of an average that we might wish to compute in the impure system.

To obtain a replica expression for A, we follow the methods of Edwards and assign each of the terms in the product (2.5a) to a different replica. Thus we produce a list of different replicas $\alpha_1, \alpha_2, \ldots, \alpha_k, \ldots, \alpha_q$. Then we replace $X_k(\sigma)$ by $X_k(\sigma^{\alpha_k})$. After a few lines of calculation, we can show that the average (2.5a) can be correctly calculated in the replica system as

$$A = \lim_{n\to 0} \frac{1}{Z(n)} \text{Tr}_{J_{ij}} \text{Tr}_{\sigma_i^\alpha} e^{-\beta H_{\text{replica}}} \times \prod_{k=1}^{q} X_k(\sigma^{\alpha_k}) \quad . \tag{2.5b}$$

For our purposes, the most important application of Eq. (2.5b) is to derive a replica expression for χ_{EA} in which Eqs. (2.5b) and (1.2) are combined to give

$$\chi_{\text{EA}} = \lim_{n\to 0} \sum_{ij} \langle \sigma_i^\alpha \sigma_i^\beta \sigma_j^\alpha \sigma_j^\beta\rangle_{(n)} \tag{2.6}$$

for α different from β, where $\langle\ \rangle_{(n)}$ is defined as the expectation value with the weights in Eq. (2.5b).

B. Gaussian probability distribution

Following Edwards, note that the simplest application of the replica method is to the case in which the probability distribution for the quenched bonds is Gaussian. In particular, if each bond is described by an independent Gaussian distribution centered upon zero, then H' in Eq. (2.1) is given by

$$\beta H' = \sum_{\langle ij\rangle} \left(\frac{J_{ij}^2}{2J_1^2} - \frac{1}{2}\ln(2\pi J_1^2) \right) \quad . \tag{2.7}$$

With this special form for H', the sum over the J's in an expression like Eq. (2.3) can be performed at once with the result

$$Z(n) = \text{Tr}_{\sigma_i^\alpha} e^{-\beta H_{\text{eff}}} \quad ,$$

where the effective spin Hamiltonian is given by

$$-\beta H_{\text{eff}} = K \sum_{\langle ij\rangle} \left(\frac{1}{2} n + \sum_{\alpha<\beta} \sigma_i^\alpha \sigma_i^\beta \sigma_j^\alpha \sigma_j^\beta \right) \quad , \tag{2.8}$$

where $\langle ij\rangle$ indicates sum over nearest neighbors and the effective four-spin constant K is

$$K = (\beta J_1)^2 \quad . \tag{2.9}$$

The effective Hamiltonian (2.8) can be treated by the same methods usually applied to nonrandom systems. The difference from the usual Ising systems is that we have here a four-spin interaction between

each pair of replicas on every bond of the lattice. This system has previously been treated by mean field theory[10,12] and renormalization methods.[5,13] We next turn to the generation of high-temperature series for this model.

C. Free-energy expansion

We employ the primitive method of series expansion[9] for the partition function arising from the Hamiltonian (2.8). (Since neither disconnected nor articulated graphs give a contribution as $n \to 0$ this approach is quite tractable.) The method employs the identity

$$e^{\pm K} = \cosh K (1 \pm \tanh K) \tag{2.10}$$

to write the partition function as

$$Z(n) = \mathrm{Tr}_{\sigma_i^\alpha} \prod_{\langle ij \rangle} e^{\frac{1}{2} K \cdot n} \prod_{\alpha < \beta} (\cosh K) \times (1 + \sigma_i^\alpha \sigma_j^\alpha \sigma_i^\beta \sigma_j^\beta \tanh K) \ . \tag{2.11}$$

Therefore all graphs possess an even number of bonds between each pair of sites. Since the trace over odd spins vanishes, each σ_i^α or site i and replica α must appear with an even power. Graphs will therefore contribute only when all vertices are even in each replica. For example in Fig. 1(b) all vertices including 2 and 5 are even in all replicas. This causes all graphs to be composed of loops, where a loop is a closed path in one replica.

From this formula a diagrammatic expansion is

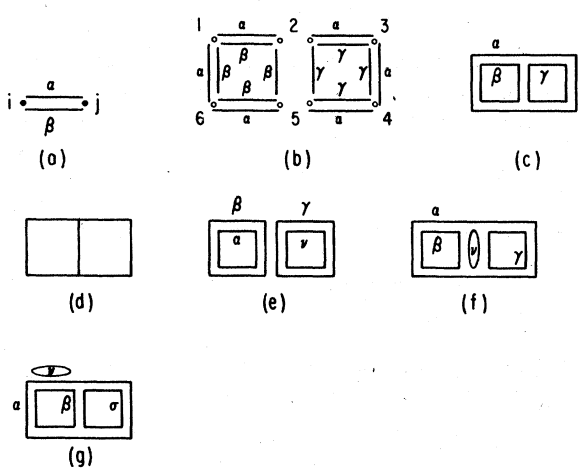

FIG. 1. Replica diagrams. (a) basic bond. (b) simple graph. (c) same graph written as loops. (d) skeleton diagram for (c), (e), (f), and (g) which are additional loop coverings of this skeleton diagram.

formed by taking the trace over all possible products of l factors $\sigma_i^\alpha \sigma_j^\alpha \sigma_i^\beta \sigma_j^\beta$ in Eq. (2.11). Each pair of replicas (α, β) can be picked only once over a bond $\langle ij \rangle$. Each such product can be represented graphically by a double line (see Fig. 1) corresponding to the basic factor $\sigma_i^\alpha \sigma_j^\alpha \sigma_i^\beta \sigma_j^\beta$.

This diagram expansion then leads to an expression for F, which arises from the $n \to 0$ limit of Eq. (2.11), in the form of a series in $\tanh K$

$$\langle F \rangle_{\mathrm{av}} = N \ln 2 + Nd(K + \ln \cosh K) + \sum_g (g) f_g \ , \tag{2.12a}$$

$$f_g = \sum_l C_{lg} \tanh^l K \ . \tag{2.12b}$$

Here N is the number of sites and Nd the number of nearest-neighbor bonds in the hypercubic lattice. The sum in Eq. (2.12a) is over the skeleton diagrams g. A skeleton diagram is one formed from an original diagram—like those in Fig. 1—by reducing all multiple bonds to single ones. The symbol (g) stands for the lattice constant for graph g, that is in how many ways it can be realized on the lattice.

Most lattice constants needed were calculated by Fisher and Gaunt[14] who kindly sent us their original list. Using the method described in that paper we calculated the three lattice constants that we need while they did not. All lattice constants needed for the free energy calculation are listed in column 2 of Table III.

The contribution of any skeleton diagram is a product of two factors: the lattice constant (g) and a statistical factor f_g. The latter is, in turn, expressed in a power series in $\tanh K$, as shown in Eq. (2.12).

To calculate the coefficients C_{lg} one needs all coverings of the skeleton graph g with $2l$ lines such that each bond is covered at least twice and all vertices are even in all replicas. Then one calculates the combinatorial expression in n which reflects the number of different ways of distributing the loops of the graph among the n replicas.

These combinatorial expressions divided by n, and then with n sent to zero, are added up for all coverings of skeleton graphs g with $2l$ lines to form C_{lg}.

Normally the primitive expansion method is encumbered by disconnected and articulated graphs. The $n \to 0$ limit here gets rid of these automatically. When a graph can be split into two subgraphs that have at most one vertex in common they share no bond or loop. Since the replica indices can then be independently picked for the two subgraphs, the weight of the graph must vanish as $n \to 0$ at least as fast as n^2. Thus, these graphs can make no contribution to a free energy calculated from Eq. (2.4). For this reason, Table III includes neither disconnected nor articulated diagrams.

Let us work through a simple diagram, i.e., the skeleton diagram given in Fig. 1(d). There is only

TABLE III. Free-energy skeleton graphs, their lattice constants and statistical factors f_g.

No.	Graph	Lattice Constant	f_g
1		d	W_o
2		$\binom{d}{2}$	$-\frac{1}{2}W_2^4 - \frac{1}{4}W_4^4$
3		$2\binom{d}{2} + 16\binom{d}{3}$	$-\frac{1}{2}W_2^6$
4	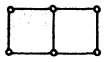	$2\binom{d}{2} + 12\binom{d}{3}$	$2W_2^7 - \frac{3}{2}W_2^6W_4 + 8W_2^3W_4^4 - 3W_2^4W_4^3$
5		$7\binom{d}{2} + 186\binom{d}{3} + 648\binom{d}{4}$	$-\frac{1}{2}W_2^8$
6		$24\binom{d}{3}$	$2W_2^8 - 3W_2^6W_4^2$
7	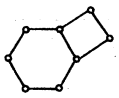	$12\binom{d}{2} + 288\binom{d}{3} + 768\binom{d}{4}$	$2W_2^9 - \frac{3}{2}W_2^8W_4$
8	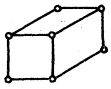	$8\binom{d}{3}$	$-4W_2^9 - 18W_2^8W_4 + 18W_2^7W_4^2$
9		$20\binom{d}{3} + 32\binom{d}{4}$	$-2W_2^9$
10	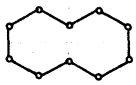	$28\binom{d}{2} + 2328\binom{d}{3} + 23136\binom{d}{4} + 47616\binom{d}{5}$	$-\frac{1}{2}W_2^{10}$
11		$4\binom{d}{2} + 312\binom{d}{3} + 1728\binom{d}{4}$	$2W_2^{10}$
12		$2\binom{d}{2} + 252\binom{d}{3} + 1152\binom{d}{4}$	$2W_2^{10}$

TABLE III. (cont'd.)

No.	Graph	Lattice Constant	f_g
13	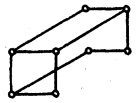	$24\binom{d}{3}$	$-4W_2^{10} - 18W_2^{9}W_4$
14		$12\binom{d}{3} + 32\binom{d}{4}$	$-17W_2^{10} + 30W_2^{9}W_4$
15		$6\binom{d}{3}$	$-8W_2^{10}$
16	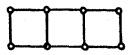	$2\binom{d}{2} + 48\binom{d}{3} + 96\binom{d}{4}$	$-8W_2^{10} + 12W_2^{9}W_4$
17		$4\binom{d}{2} + 72\binom{d}{3} + 192\binom{d}{4}$	$-8W_2^{10} + 12W_2^{9}W_4$
18	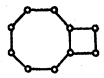	$48\binom{d}{2} + 3744\binom{d}{3} + 32448\binom{d}{4} + 51840\binom{d}{5}$	$2W_2^{11}$
19	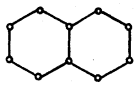	$14\binom{d}{2} + 1392\binom{d}{3} + 10656\binom{d}{4} + 15360\binom{d}{5}$	$2W_2^{11}$
20	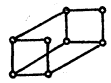	$12\binom{d}{3}$	$8W_2^{11}$
21		$96\binom{d}{3} + 384\binom{d}{4}$	$-8W_2^{11}$
22	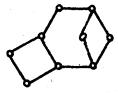	$96\binom{d}{3} + 384\binom{d}{4}$	$-8W_2^{11}$
23	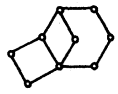	$192\binom{d}{3} + 768\binom{d}{4}$	$-8W_2^{11}$

TABLE III. (cont'd.)

No.	Graph	Lattice Constant	f_g
24	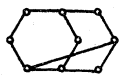	$48\binom{d}{3} + 192\binom{d}{4}$	$-4W_2^{11}$
25	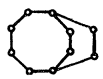	$612\binom{d}{3} + 5856\binom{d}{4} + 3840\binom{d}{5}$	$2W_2^{11}$
26	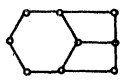	$4\binom{d}{2} + 168\binom{d}{3} + 768\binom{d}{4}$	$-4W_2^{11}$

one way it can be covered so that two lines appear on each bond of the skeleton graph, namely as shown in Fig. 1(c). Since all seven lines are covered twice this graph is proportional to $(\tanh K)$.[7] Since $(\alpha\beta)$, $(\alpha\gamma)$, and $(\beta\gamma)$ all form bonds [see Fig. 1(b)] each index must refer to a distinct replica. Thus there are $n(n-1)(n-2)$ ways of picking these replica indices. To form C_{7g}, one must divide this number by n [see Eq. (2.4)] and take n to zero. The result is that for this graph $C_{7g}=2$.

Exactly this same mode of analysis serves to evaluate all contributions to the skeleton graphs shown in Table III. However, the analysis outlined so far is somewhat time consuming because in higher order many, many coverages of the skeleton graph need to be considered. For example, Fig. 1(e) – 1(g) list three of the eight coverages needed to get the eighth-order contribution to this graph. Fortunately this labor can be considerably reduced by the method of bond renormalization described in Sec. II D.

D. Bond renormalization

Figures 1(e) – 1(g) are all of eighth order in $\tanh K$. However Figs. 1(f) and 1(g) differ from Fig. 1(e) in that they contain two identical replica indices (i.e., ν) on a single bond. All diagrams in which there appear such closed loops on a single bond can be replaced by lower order diagrams in which the basic bonds are renormalized.

The basic point in this replacement is that whenever a closed loop appears on a single bond, this loop does not affect the evaluation of the rest of the diagram. Therefore, one can isolate each basic bond and calculate the loop renormalizations for each bond separately. The resulting renormalized bond will have a value W_m, which depends only upon the number of unpaired—i.e., distinct—replica indices which appear on it. For example, Fig. 2 describes a diagrammatic expansion of W_2. Here α and β are considered fixed and distinct. The first term has a weight which is simply $\tanh K$, reflecting the single way α and β can be paired to form a basic four spin factor on the bond. For the next term, ν can be picked in $(n-2)$ ways so as to be distinct from α and β. The only possible pairing is $(\alpha\nu)(\beta\nu)$. Hence at $n=0$ this term is $-2(\tanh K)^2$. The next term permits the pair $(\nu\lambda)$ to be picked in $\frac{1}{2}(n-2)(n-3)$ ways. Since ν and λ appear symmetrically, there are two distinct pairings, namely $(\alpha\nu)(\nu\lambda)(\lambda\beta)$ and $(\alpha\lambda)(\lambda\nu)(\nu\beta)$ so that this term has the value $+6(\tanh K)^3$. In summary we have

$$W_2=\tanh K-2(\tanh K)^2+6(\tanh K)^3+\cdots\ . \quad (2.13a)$$

A very similar renormalization may be applied to a diagram containing a bond with four distinct lines as

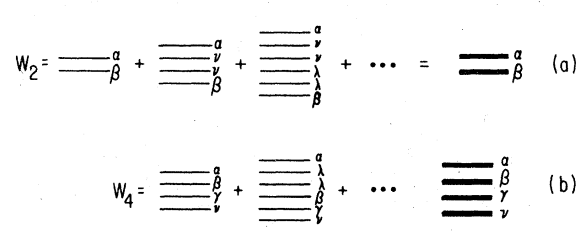

FIG. 2. Bond renormalization.

in Fig. 2(b) to give a renormalized four replica bond as

$$W_4 = 3(\tanh K)^2 - 12(\tanh K)^3 + \cdots \quad . \tag{2.13b}$$

Notice that these W's are exactly the same as the one-bond averages calculated in Eq. (1.5). This is because we can see that $W_m = \langle \sigma_i^{\alpha_1} \cdots \sigma_i^{\alpha_m} \sigma_j^{\alpha_1} \cdots \sigma_j^{\alpha_m} \rangle_0$ where $\langle\ \rangle_0$ is as in Eq. (1.5) the average in the replicated system with only two sites i and j. Now using Eq. (2.5), the identity to Eq. (1.5) can be easily established. Hence by using the bond renormalization, one is essentially converting the series in $\tanh K$ into a series in the W's.

For the purpose of generating the series, one might wish to see the W's expressed as power series in the variable

$$K = \langle (\beta J)^2 \rangle_{\text{av}} \quad .$$

This is actually most conveniently done via Eq. (1.5) which gives

$$W_{2m} = \sum_{l=m}^{\infty} K^l A_{m,l} B_l \quad . \tag{2.14}$$

Here B_l are the renormalized moments

$$B_l K^l = \langle (\beta J)^{2l} \rangle_{\text{av}} \tag{2.15}$$

and $A_{m,l}$ are the coefficients of a power series expansion of $[\tanh(x)^{1/2}]^{2m}$ in x. In the Gaussian case, we have

$$B_l = \frac{(2l-1)!}{2^{l-1}(l-1)!} \quad . \tag{2.16}$$

Now return to the skeleton diagram in Fig. 1. The bond-renormalized forms of diagrams 1(c) and 1(e) are shown in Figs. 3. The diagram in Fig. 3(a) includes the unrenormalized diagrams 1(f) and 1(g) and five more (identical) eighth-order terms. The net result is that Fig. 3(a) has the value $2W_2^7$, Fig. 3(b) has the value $-\frac{3}{2}W_2^6 W_4$. Thence the sum of these contributions

$$C_{lg}(\tanh K)^l = 2W_2^7 - \tfrac{3}{2} W_2^6 W_4 + \cdots$$

includes all contributions to the skeleton diagram up to the order $l = 9$. This renormalization is indeed a relatively efficient tool for handling the coverages of these skeleton diagrams.

Table III lists in its last column the evaluation of each of the diagrams in a multinominal in the W's including all terms up to order $(\tanh K)^{11}$. Our derivation only applies to a Gaussian $P(J)$. In the next chapter, we show that the data in Table III is equally correct for any symmetrical $P(J)$. The diagrams in Table III are summed up to give Table I which summarizes the free-energy series.

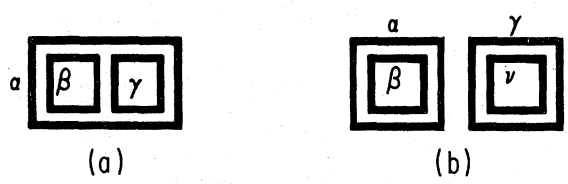

FIG. 3. Renormalized diagrams.

Susceptibility series

The expression (2.6) for the Edwards-Anderson susceptibility can be evaluated by applying the same ideas. The basic diagrams contain two distinguished points, at the i, j spin sites. The indices α and β do not appear in closed loops but instead flow over lattice bonds from one dot to the other. All other replica indices occur in closed loops.

Figure 4 shows some of the low-order diagrams and an evaluation of the statistical factor for each graph through order K^{10}. The graphs which do not have closed loops have the trivial statistical factor

$$f_g = (W_2)^l \quad ,$$

where l is the number of bonds in the skeleton graph. Similar, but more complicated, evaluations apply to the other diagrams.

For reasons which will be apparent below, we are especially interested in skeleton diagrams which can give a factor f_g that includes a contribution proportional to W_6 among its terms of 10th order or below.

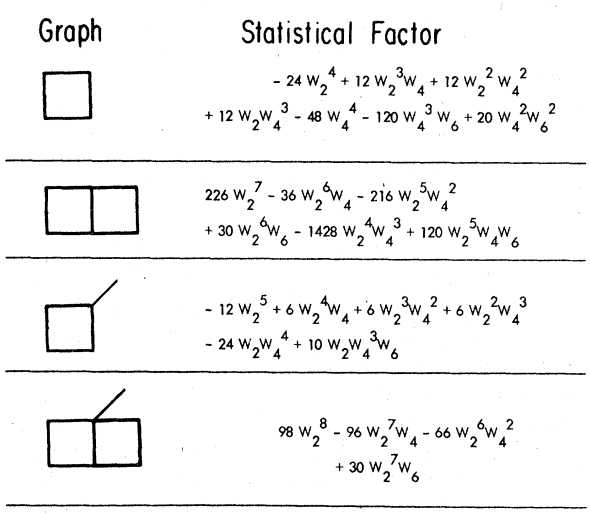

FIG. 4. Susceptibility graphs with W_6.

Figure 4 shows all diagrams in the Fisch list which can contribute such a W_6 term. In Sec. III, we shall use these data in conjunction with the data of Fisch[1] to generate the susceptibility series described in Table II.

III. LINKED-CLUSTER EXPANSIONS

The basic approach in the linked-cluster method is to expand a physical quantity, like the free energy, in a series of terms each of which depends upon the couplings in some small connected region of the lattice. After this expansion is performed, the individual terms in the expansion are each averaged over the probability distribution of the couplings.

A. Setting up the free-energy expansion

To illustrate this method, consider the free energy

$$\langle F\rangle_{\rm av} = \langle \ln \sum_{\sigma_i} \prod_{\langle ij\rangle} e^{\beta J_{ij}\sigma_i\sigma_j}\rangle_{\rm av} \ . \tag{3.1}$$

By using Eq. (2.10), one can express the free energy in terms of

$$T_{ij} = \tanh(J_{ij}/kT) \ . \tag{3.2}$$

The alternative writing is

$$\langle F\rangle_{\rm av} = N\ln 2 + NdW_0 + F_c \ . \tag{3.3}$$

W_0 is defined in Eq. (1.3) and the correlated part of the free energy is given by

$$\langle F_c\rangle_{\rm av} = \langle \ln \frac{1}{2^N} {\rm Tr}_\sigma \prod_{\langle ij\rangle} (1+\sigma_i T_{ij}\sigma_j)\rangle_{\rm av} \ .$$

Here the average over spin values can be formally evaluated as

$$\langle F_c\rangle_{\rm av} = \langle \ln(1+\sum_\alpha P_\alpha)\rangle_{\rm av} \ . \tag{3.4}$$

Now P_α represents a product of T_{ij} over closed loops in the lattice just like the replica loops considered in Sec. II. The sum over α is a sum over all such closed loops.

To evaluate the sum in Eq. (3.4) it is convenient to expand the logarithm in the form of a multinominal expansion in which the loop product P_α is raised to the power n_α. The list of all n_α's is called a *loop coverage* and is described by a vector $n=(n_1, n_2,\ldots, n_\alpha,\ldots)$. The free energy is then given by

$$F_c = \sum_{\vec{n}} C(\vec{n}) \prod_\alpha P_\alpha^{n_\alpha} \ , \tag{3.5}$$

where the coefficients in the sum are

$$C(\vec{n}) = (-1)^{n_T-1}(n_T-1)! \prod_\alpha \frac{1}{n_\alpha!} \tag{3.6}$$

with n_T being the total number of loops and therefore nonzero while the n_α are nonnegative integers and

$$n_T = \sum_\alpha n_\alpha \ . \tag{3.7}$$

Notice the structure of the expansion (3.5). On each bond, we find a power of T_{ij}, T_{ij}^m, which becomes W_m of Eq. (1.5) after averaging. Then Eq. (3.5) becomes an expansion in powers of W_1, W_2, $W_3,\ldots$ When the symmetry (1.1) holds the W_m vanish for odd m.

Each term in Eq. (3.5) can be represented as a graph formed by loops in which n_α represents the number of times the αth loop is covered. To make further progress, we collect together all the different terms in Eq. (3.5) which cover a given skeleton graph.

To evaluate the contribution of a skeleton graph we consider the graph to be a small system for which the free energy can be calculated by applying Eq. (3.5). The formula for the graph evaluation is then identical to Eq. (3.5) except that only a limited number of loops (with indices $\alpha=1,2,\ldots,N_L$) need be taken into account. The net result is that the value of a graph is given by

$$f_g = \sum_n{}' \prod_{\alpha=1}^{N_L} \langle P_\alpha^{n_\alpha}\rangle_{\rm av} C(\vec{n}) \ . \tag{3.8}$$

The prime on the sum is intended to indicate that the sum includes only those loop coverages which actually go over *all* bonds in the graph. If one or more bonds is uncovered, the term is not included in Eq. (3.8) because the contribution has already been included in a lower order skeleton diagram. N_L is the number of loops in the coverage.

We can thus conclude Sec. III A by writing our result for the free-energy series as a sum over skeleton graphs of the form

$$\langle F_c\rangle_{\rm av} = \sum_g (g) f_g \ . \tag{3.9}$$

As before, (g) is a lattice constant which describes in how many ways a given skeleton graph may be fit onto the lattice. Then f_g is a statistical factor which

describes how a given graph contributes to the free energy. We describe the evaluation of f_g in Sec. III B.

B. Graph evaluation technique

The statistical factors f_g, must be evaluated separately for each graph topology. To begin with, consider the simple one-loop topology like that given in Fig. 5(a). In this graph only one loop is possible, that being a product of l T_{ij}'s—where l is the number of bonds in the skeleton graph. From Eqs. (3.4) or (3.8), we can evaluate this graph as

$$\begin{aligned} f_g &= \langle \ln(1+P)\rangle_{\rm av} \\ &= \sum_{m=1}^{\infty} \frac{(-1)^{m-1}}{m} \langle P^m \rangle_{\rm av} \\ &= \sum_{m=1}^{\infty} \frac{(-1)^{m-1}}{m} (W_m)^l \ . \end{aligned} \tag{3.10}$$

A two-loop, or θ graph, like that shown in Fig. 5(d) can be evaluated in much the same manner. As a guide to more complex graphs, we describe this graph in a topological fashion as shown in Fig. 6. Let a *topological vertex* be a point where three or more bonds come together. Let a *branch* denoted by a latin index i be a line consisting of l_i bonds which either

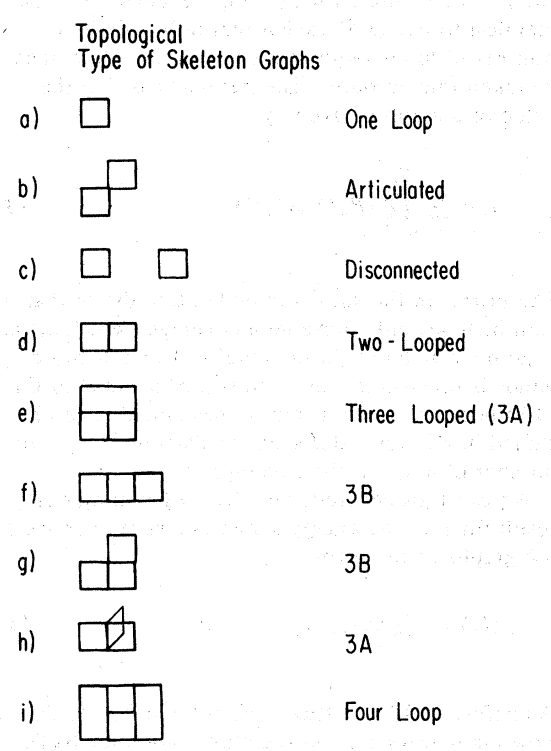

FIG. 5. Types of topological skeleton graphs.

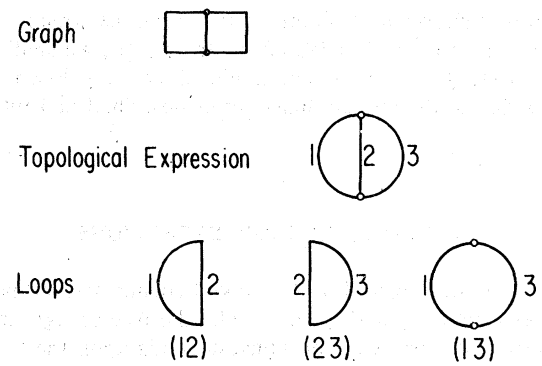

FIG. 6. Two-loop graph.

forms a full loop (as in the one-loop diagram) or connect two topological vertices. The skeleton diagram in question has two topological vertices and three branches, labeled $i=1,2,3$, which have respectively $l_1=3$, $l_2=1$, $l_3=3$. The skeleton diagram admits three loops labeled respectively with $\alpha=(12)$, $\alpha=(23)$, and $\alpha=(13)$ and has the statistical factor

$$f_g = \sum_{n_{12},n_{13},n_{23}}{}' C(\vec{n}) \langle P_{12}^{n_{12}} P_{13}^{n_{13}} P_{23}^{n_{23}} \rangle_{\rm av} \ .$$

The prime on the sum is a reminder that we cannot include the already-counted one-loop terms. Thence two of the three n's must be nonzero. An evaluation of the averages then gives

$$f_g = \sum_{n_{12},n_{13},n_{23}}{}' C(\vec{n}) \prod_{i=1}^{3} [W_{m_i(n)}]^{l_i} \tag{3.11}$$

with $m_i(\vec{n})$ being the number of times the ith branch is covered, i.e.,

$$m_i(n) = \sum_{j \neq i} n_{ij} \ . \tag{3.12}$$

To depict the different loop coverages, we draw the loops onto the topological diagram as shown in Fig. 1(c) and (e).

Higher order graphs are evaluated in exactly the same manner as described here. This evaluation is simplified by the fact that disconnected diagrams, like those in Fig. 5(c), and articulated diagrams, like those in Fig. 5(b) vanish.

To see how this happens consider a disconnected diagram like that in Fig. 7. According to Eq. (3.4) the total free energy which might result from such a diagram is

$$\begin{aligned} f_g = \langle &\ln(1+P_a+P_b+P_{ab}) \\ &-\ln(1+P_a)-\ln(1-P_b)\rangle_{\rm av} \ . \end{aligned} \tag{3.13}$$

The subtraction terms in Eq. (3.13) appear to eliminate the contributions from the already-calculated

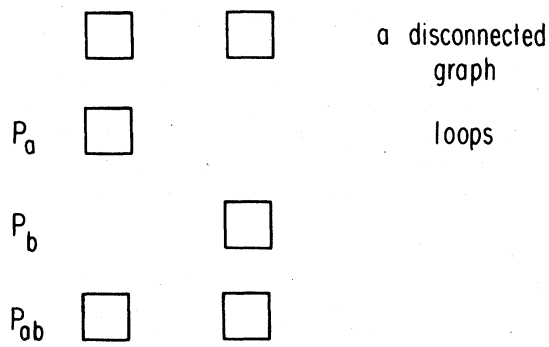

FIG. 7. Disconnected diagram.

single-loop terms. But for disconnected or articulated diagrams $P_{ab} = P_a P_b$ so that the argument of the first logarithm in Eq. (3.13) factorizes and the entire right-hand side cancels out.

Expressions like Eq. (3.11) give a useful but cumbersome evaluation of the statistical factor for a given graph. However, a better form can be obtained if we use the concept of branch coverages, i.e., the set of integers $\vec{m} = (m_1, m_2, \ldots, m_{N_B})$ which describe how many times a given branch in the diagram has been covered. For a general skeleton graph containing N_B branches which respectively contain a number of bonds $l_1, l_2, \ldots, l_{N_B}$, one can write the statistical factor as

$$f_g = \sum_{\vec{m}} a_g(\vec{m}) \prod_{i=1}^{N_B} (W_{m_i})^{l_i} \quad . \tag{3.14}$$

The sum over m's include all values of m_i from 1 to ∞. The factors $a_g(\vec{m})$ described in the Appendix give the statistical weight of a given branch coverage. They depend only upon the topology of the graph.

C. Free-energy series

The data in Fig. 8 is sufficient to enable one to calculate a free-energy series based upon all the star graphs with 11 or fewer bonds which can be fit onto hypercubic lattices. These graphs are shown in Table III. To get an 11th-order series, we note that W_{2n} is of order K^n. In Table III, we list the graph, its lattice constant and all contributions to the graph up to order K^{11}. For example, skeleton graph number 4 is of the two-loop type with $l_1 = 3$, $l_2 = 1$, $l_3 = 3$. The necessary branch coverages are then listed in Table IV as are the contributions to f_g [as given in Eq. (3.14)]. Thus, as shown in Table III the total contribution from this graph is

$$f_g = 2W_2^7 - \tfrac{3}{2} W_2^6 W_4 - 3W_2^4 W_4^3 + 8W_2^3 W_4^4 \quad . \tag{3.15}$$

For comparison one can look at the result of Fisch for this graph in the case of a double delta-function distribution

$$P(J) = \tfrac{1}{2}\delta[J - kT(K)^{1/2}] + \tfrac{1}{2}\delta[J + kT(K)^{1/2}] \quad , \tag{3.16}$$

for which

$$W_2 = [\tanh(K)^{1/2}]^2 \tag{3.17}$$

topological form of graph	branch coverages higher than two	$a_g(m)$
single loop	none	-1/2
	n = 4	-1/4
Graphs 2, 3, 5, 10		
two loop	none	2
	one n equals 4	-3/2
	two n's equal 4	4
	one n equals 6	0
Graphs 4, 6, 7, 9, 11 12, 18, 19, 25	one n equals 8	0
3 A	none	-17
	one n equals 4	30
Graph 14		

topological form of graph	branch coverages higher than two	$a_g(m)$
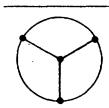 3 B	none	- 4
	one n equals 4	- 6
	two n's equal 4	12
Graphs 8, 13, 24, 26	one n equals 6	0
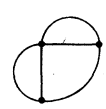 3C	none	- 8
	n_1 or n_2 or n_4 or n_5 equals 4	6
Graphs 15, 16, 17, 21, 22, 23		
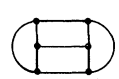 4 loop	none	8
Graph 20		

FIG. 8. Evaluation of topological constants for all free-energy graphs to the 11th order.

TABLE IV. Calculation of f_g for skeleton graph number 4.

branch coverages $m=m_1,m_2,m_3$	contribution of f_g
2,2,2	$2W_2^7$
2,4,2	$-\frac{3}{2}W_2^6W_4$
4,2,2	$-\frac{3}{2}W_2^4W_4^3$
2,2,4	$-\frac{3}{2}W_2^4W_4^3$
4,4,2	$4W_2^3W_4^4$
2,4,4	$4W_2^3W_4^4$
2,6,2	0
2,8,2	0
2,10,2	0

and

$$W_4 = W_2^2 \ . \tag{3.18}$$

Fisch's result for this diagram is

$$f_g = 2W_2^7 - \tfrac{3}{2}W_2^8 - 3W_2^{10} \tag{3.19}$$

which, of course, checks the correctness of our result, except for the last term. In fact, we could have obtained the first three terms in Eq. (3.15) by using Fisch's result, (3.19), and then recognizing that each term must have the structure $W_2^{q_1}W_4^{q_2}$ where q_1 and q_2 must add up to the number of bonds (i.e., 7).

Not only does this kind of comparison serve as a very detailed check of our work, but it will enable us to infer the form of the susceptibility series for a general $P(J)$, based upon Fisch's calculation, which was restricted to the form (3.16).

The data in Table III permits us to calculate 11th-order free-energy series in the form

$$F_c = \sum_{p_2,p_4,q} c^q_{p_2,p_4} \binom{d}{q} W_2^{p_2} W_4^{p_4} \ . \tag{3.20}$$

This form of F does not include terms of the form $W_6^{p_6}$ because these terms cannot contribute at any order lower than K^{12}. Table I lists the coefficients $c^q_{p_2,p_4}$ required up through the 11th order.

The series for the case of the double-delta distribution given in Eq. (3.18) is obtained by setting $W_4 = W_2^2$. The first ten terms are identical to Fisch and Harris, apart from an unexplained factor of 2 in their series already noted by Cheery and Domb. The 11th term is new.

D. Susceptibility series

The same general mode of analysis would enable us to obtain a series for the Edwards-Anderson susceptibility χ_{EA} in the form (1.6b). Through order K^{10} only terms involving W_2, W_4, and W_6 appear.

Fisch and Harris have calculated all graphs in this susceptibility series for the distribution (3.1). As explained in Sec. III C, if only W_2 and W_4 were involved, we could simply write down the form of the coefficients a^q via a small reinterpretation of the data presented by Fisch. However four of the skeleton graphs analyzed by Fisch lead to contributions involving W_6. In Fig. 4, we calculated these four graphs. Thus by using these results and borrowing the results of Fisch and Harris, we can realize a 10th order susceptibility series of the form (1.6b) for a general distribution.

E. Preliminary analysis

We have looked at the series generated by the Gaussian distribution. Apparently the susceptibility series behaves in a very similar way to that of the double delta analyzed by Fisch and Harris. The derived indices and even the B-value are very much the same as in this earlier work. However, to our surprise the specific-heat series shows some signs of interesting critical behavior for the Gaussian distribution but not for the double delta. More definitive analysis will appear in a future publication.

ACKNOWLEDGMENTS

We would like to thank A. Aharony for suggesting the problem, J. H. Gibbs for helpful discussions, R. Fisch for sending us a copy of his thesis and helpful additional unpublished material, and M. E. Fisher for the list of lattice constants and helpful advice. The work was partly supported by the Materials Research Laboratory at Brown University, funded by the NSF, and by United States Public Health Service Grant No. GM 10906-18. Also supported by NSF Grant No. DMR 77-12637.

APPENDIX: EXAMPLE OF EVALUATION OF THE TOPOLOGICAL FACTOR $a_g(m)$ USING BRANCH COVERAGE

Generally, a given branch coverage can be realized via several loop coverages. Correspondingly, the factors $a_g(\vec{m})$ are computed [via Eq. (3.8)] as a sum over the weights for those loop coverages which real-

TABLE V. Values of v_i^α.

branch index i	loop index α: 0	(1,2)	(1,3)	(1,4)	(2,3)	(2,4)	(3,4)
1	1	1	1	1	0	0	0
2	1	1	0	0	1	1	0
3	1	0	1	0	1	0	1
4	1	0	0	1	0	1	1

ize the branch coverage m. In symbols, we have

$$a_g(\vec{m}) = (\sum_{\vec{n}}) C(n) \prod_i \delta_{m_i, m_i(n)} \quad . \tag{A1}$$

Here $m_i(\vec{n})$ is the branch coverage expressed as a function of the loop coverage. In general, $m_i(n)$ is the sum of all n_α's which describe loops which cover the branch i. In symbols, we have

$$m_i(n) = \sum_\alpha v_i^\alpha n_\alpha \tag{A2}$$

with

$$v_i^\alpha = \begin{cases} 1 & \text{if loop } \alpha \text{ goes over branch } a \\ 0 & \text{otherwise} \end{cases} \quad . \tag{A3}$$

In this way, the graph evaluation has been reduced to the topological problem of finding the coefficients $a_g(\vec{m})$. However, before we attack this problem, we should notice an extra simplification which applies to the spin-glass case: The graph vanishes unless all the m's are even.

Equations (A1), (A2), and (A3) give all the information needed to calculate the statistical factor for each skeleton graph. Let us describe in some detail how the topological weight factors $a_g(\vec{m})$ may be calculated as a function of the graph topology and the coverage $\vec{m}$.

Consider, for example, the evaluation of the topological factors for the graph labeled 3A in Fig. 8. This graph has four branches labeled with $i = 1, 2, 3, 4$ in the figure and can be covered by seven loops, which we label by $\alpha = 0$ (being the loop which covers all the branches) and $\alpha = (i,j)$ (being the loop which covers branches i and j). Then the v_i defined by Eqs. (A3) are given in Table V.

In our example, we calculate the loop indices which correspond to the branch coverage: $m = (4, 2, 2, 2)$. Then one can write a small computer program to solve Eq. (A2) for the m's given the n's. The solution is not unique; all solutions are given in Table VI. This table also gives the weights $C(m)$, corresponding to the four possible loop coverages. The sum of these weights is 30, which is the topological factor $a_g(\vec{m})$ listed in Fig. 8.

TABLE VI. Loop coverings corresponding to $\vec{m} = (4, 2, 2, 2)$.

solution number	values of m_α: $\alpha = 0$	(1,2)	(1,3)	(1,4)	(2,3)	(2,4)	(3,4)	weight $C(\vec{m})$
1	1	1	1	1	0	0	0	−6
2	0	2	1	1	0	0	1	12
3	0	1	2	1	0	1	0	12
4	0	1	1	2	1	0	0	12

[1]R. Fisch, Ph.D thesis (University of Pennsylvania) (unpublished).
[2]R. Fisch and A. B. Harris, Phys. Rev. Lett. 38, 785 (1977).
[3]R. J. Cherry and C. Domb, J. Phys. A 11, L5 (1978).
[4]S. F. Edwards and P. W. Anderson, J. Phys. F 5, 965 (1975).
[5]A. B. Harris, T. C. Lubensky, and J. H. Chen, Phys. Rev. Lett. 36, 415 (1976).
[6]P. W. Anderson and C. M. Pond, Phys. Rev. Lett. 40, 903 (1978).
[7]P. W. Southern and A. P. Young, J. Phys. C 10, 2179 (1977).
[8]S. F. Edwards, in Proceedings 3rd Conference on Amorphous Matter, 1970 (unpublished).
[9]C. Domb and M. Green, ed., *Phase Transitions and Critical Phenomena,* (Academic, New York, 1974) Vol. III.
[10]D. Sherrington and S. Kirkpatrick, Phys. Rev. Lett. 35, 1792 (1975).
[11]J. R. L. de Almeida and D. J. Thouless, J. Phys. A 11, 983 (1978).
[12]D. J. Thouless, P. W. Anderson and R. G. Palmer, Philos. Mag. 35, 593 (1977).
[13]C. Jayaprakash, J. Chalupa and M. Wortis, Phys. Rev. B 15, 495 (1977).
[14]M. E. Fisher and D. S. Gaunt, Phys. Rev. 133, A224 (1964).